Wave packet collisions in Yang-Mills-Higgs theory

C. R. Hu, S. G. Matinyan,* B. Müller, and D. Sweet†
Department of Physics, Duke University, Durham, North Carolina 27708-0305
(Received 15 September 1995; revised manuscript received 30 November 1995)

We present numerical simulations of colliding wave packets in spontaneously broken SU(2) Yang-Mills-Higgs theory. Compared with pure Yang-Mills theory, introducing the Higgs field leads to new aspects in the dynamics of the system. The evolution of the gauge field and the Higgs field is investigated as a function of the amplitude of the wave packets and of the mass ratio of the Higgs boson and the gauge boson. We find regions in our parameter space in which initial wave packets scatter into final configurations with dramatically different momentum distributions.

PACS number(s): 11.15.Kc, 02.60.Cb, 13.85.Hd

I. INTRODUCTION

Collisions between classical wave packets have recently been studied numerically for several interacting relativistic field theories [1–4]. Interest in this topic arose in connection with expectations that the rate of multiparticle production processes in electroweak interactions, which can manifest themselves, e.g., in baryon-number violation, might be unsuppressed at high energies [5].

The nonperturbative nature of the baryon-number-violating amplitude [6] demands a corresponding nonperturbative approach as provided by semiclassical techniques. The main difficulty in semiclassical approaches is the treatment of the $2\rightarrow$ many particle transition amplitude, since the *initial* state of high energy particles is not semiclassical at all, and loop contributions are essential in general (see, e.g., [7]). Possible techniques for circumventing this difficulty of the semiclassical approach have been proposed and studied in the literature [8–10].

In the classical approach to scattering, the question is the following: Does there exist a mechanism for energy transfer from high frequency modes, which corresponds to two high energy particles, to low frequency modes representing a multiparticle final state? At first glance, the answer to the question, formulated in terms of nonlinear dynamics, seems to be affirmative since the gauge field theories are nonlinear. However, the studies of $(1+1)$-dimensional Abelian Higgs model [1] and $\lambda\varphi^4$ theory [2] have shown no indication for a nonperturbative mechanism providing the coupling between the initial high and the final low frequency modes. For example, in [1] the wave packets always passed through each other without being destroyed. It is important to note that in [1] the initial states were always chosen to have small amplitudes, which made the nonlinear terms less important.

The important issue here is that the results are strongly influenced by the nonlinearity because of the non-Abelian spin-field coupling, which is absent in Abelian models. It is this coupling that is responsible for the infrared instabilities of the pure non-Abelian gauge theory. This can be seen from the linearized equation describing small perturbations a_μ^c around an SU(2) background field A_μ (in background gauge):

$$(D_\mu^2 a_\nu)^a - 2g\varepsilon^{abc}F_{\mu\nu}^b a_\mu^c = 0, \tag{1}$$

where $D_\mu \equiv \partial_\mu - ig[A_\mu,]$ is the gauge-covariant derivative. The second term in (1) may have any sign. In particular, this essentially non-Abelian coupling drives an instability for perturbations with isospin polarization orthogonal to the isospin of a standing wave, which leads to a growth of low frequency modes from initial high frequency modes [3]. This may imply the existence of classical trajectories of the type required for multiparticle production [9], if the instability persists in more realistic cases, e.g., collisions of localized gauge field wave packets.

From a more general point of view, the observed inability of the nonlinearity to furnish a mechanism for the formation of strongly inelastic final states is, in our opinion, intimately connected with the integrable nature of the classical systems considered in [1] and [2]. It is well known that non-Abelian gauge theories are nonintegrable in the classical limit , and exhibit dynamical chaos [11,12].[1] This dynamical stochasticity of the non-Abelian gauge fields together with their mentioned dynamical instability are possible sources of the nonperturbative mechanism for the coupling between high and low frequency modes. At the same time, it is important to recall the special role of the Higgs field as a mechanism for the suppression of the dynamical chaos of the non-Abelian gauge fields [13].

With this in mind, we studied [4] the collision of two SU(2) gauge field wave packets, homogeneous in the transverse plane. As we expected, based on previous results [3], the collision of essentially non-Abelian initial configurations trigger the decay of initial high frequency modes into many low frequency modes with dramatically different momentum

*On leave of absence from Yerevan Physics Institute, Yerevan, Armenia.

†Present address: Physics Department, Boston University, Boston, MA 02215.

[1]Strictly speaking, chaos only sustains for solutions of finite energy *density* [12]. Finite energy solutions in 3+1-dimensions will spread out in space at late times and will therefore linearize. However, numerical results indicate that at intermediate times these fields generally exhibit exponentially growing perturbations.

distributions, whereas for Abelian configurations (parallel relative isospin polarizations) wave packets pass through each other without interaction.

The present paper, which studies collisions of wave packets in the SU(2) Higgs model, is a generalization of the earlier work in two directions. First, it is an extension of [1] to the non-Abelian Higgs model. Second, it is a generalization of the previous work [4] to the case where the SU(2) gauge symmetry is spontaneously broken by a Higgs field and the fundamental excitations of the gauge field are massive.

One expects that the explicit mass scale introduced by the Higgs field will act as a cutoff on the low frequency excitations, potentially leading to drastic changes in the coupling between high and low frequency modes. We will see that the real situation is more complicated, and the ratio λ/g^2 of the Higgs self-coupling λ and gauge coupling g and the vacuum expectation value v of the Higgs field are essential parameters.

This paper is organized as follows. In Sec. II, we formulate the problem. In Sec. III, we present results from our numerical simulations and discuss their implications. Section IV is devoted to an extended discussion of our results. In Sec. V, we conclude and indicate possible directions for future research.

II. FORMULATION OF THE PROBLEM

In this section, we describe scattering of classical wave packets in the non-Abelian Higgs model and its numerical formulation on the lattice. In particular, we give a brief discussion of the scaling properties of the classical dynamics. This section is based on previous work [1,4].

A. The non-Abelian Higgs model

Here we give a brief discussion of the spontaneously broken SU(2) Yang-Mills theory, in which a charged scalar isodoublet field, the Higgs field, is coupled to the gauge field. This model retains the most relevant ingredients of the electroweak theory. The action describing this model in 3+1 dimensions is given by

$$S=\int d^3x\,dt\left\{-\frac{1}{2}\mathrm{tr}(F_{\mu\nu}F^{\mu\nu})+\frac{1}{2}\mathrm{tr}[(D_\mu\Phi)^\dagger D^\mu\Phi]-\lambda\left[\frac{1}{2}\mathrm{tr}(\Phi^\dagger\Phi)-v^2\right]^2\right\} \tag{2}$$

with $D_\mu=\partial_\mu-igA_\mu^a\tau^a/2$, $F_{\mu\nu}\equiv F_{\mu\nu}^a\tau^a/2=(i/g)[D_\mu,D_\nu]$, and

$$\Phi=\phi^0-i\tau^a\phi^a, \tag{3}$$

where τ^a $(a=1,2,3)$ are Pauli matrices. Following the notation of [14], we represent the complex Higgs doublet by a quaternion, which is convenient for numerical manipulation. Clearly, this maintains the correct number of degrees of freedom in the Higgs field.

By a scaling transformation

$$x'_\mu=gvx_\mu,\quad \Phi'=\Phi/v,\quad A'_\mu=A_\mu/v, \tag{4}$$

we obtain the action in terms of the primed quantities

$$S=(1/g^2)\int d^3x'\,dt'\left\{-\frac{1}{2}\mathrm{tr}(F'_{\mu\nu}F'^{\mu\nu})+\frac{1}{2}\mathrm{tr}[(D'_\mu\Phi')^\dagger D'^\mu\Phi']-\lambda'\left(\frac{1}{2}\mathrm{tr}(\Phi'^\dagger\Phi')-1\right)^2\right\} \tag{5}$$

with $\lambda'=\lambda/g^2$.

Within classical physics, the prefactor $1/g^2$ in (5) is irrelevant, leaving $\lambda'=\lambda/g^2$ as the only relevant parameter in the action. Note that λ' is proportional to the square of M_H/M_W, the mass ratio of the Higgs boson and W boson.

The elementary excitation modes ρ and W_μ are best described in the unitary gauge

$$\Phi=(v+\rho/\sqrt{2})U(\theta), \tag{6}$$

$$A_\mu=U(\theta)W_\mu U^{-1}(\theta)-(1/ig)[\partial_\mu U(\theta)]U^{-1}(\theta), \tag{7}$$

where $U(\theta)=\exp(i\tau^a\theta^a)$, ρ describes oscillation of the Higgs field about its vacuum expectation value, and W_μ is the field of the gauge boson. W_μ and ρ obey the classical equations of motion

$$[D_\mu,F^{\mu\nu}]+M_W^2W^\nu+\frac{1}{\sqrt{2}}g^2v\rho W^\nu+\frac{1}{4}g^2\rho^2W^\nu=0, \tag{8}$$

$$(\partial_\mu\partial^\mu+M_H^2)\rho+3\sqrt{2}\lambda v\rho^2+\lambda\rho^3-\frac{\sqrt{2}}{4}g^2vW_\mu^aW^{a\mu}-\frac{1}{4}g^2\rho W_\mu^aW^{a\mu}=0, \tag{9}$$

where $M_H=2v\sqrt{\lambda}$ and $M_W=gv/\sqrt{2}$. D_μ and $F^{\mu\nu}$ are defined in terms of W_μ. After a scaling transformation similar to that in (4), it is easy to see that the above equations of motion depend on a single parameter: the mass ratio M_H/M_W. However, in the simulation of colliding wave packets, there are other parameters involved in the initial condition.

B. Scattering of classical wave packets

Our numerical study is based on the Hamiltonian formulation of lattice SU(2) gauge theory [15] (see [4,16] for more details), in which the dynamic variables are link variables defined as

$$U_\ell=\exp(-igaA_\ell^c\tau^c/2), \tag{10}$$

where ℓ stands for the link index. As in [4], we work on a one-dimensional lattice with a physical size $L=Na$, where N is the number of lattice sizes and a the lattice spacing. We arrange initially two Gaussian wave packets with average momenta $\mathbf{k}=(0,0,\bar{k})$, and width Δk. Our goal is to simulate the collision of two W-boson wave packets in the background of the Higgs condensate.

Before actually constructing the wave packets, one has to deal with the gauge-fixing problem. In the Hamiltonian formulation of lattice gauge theory, temporal gauge $A_0=0$ is most convenient. On the other hand, one must construct the

W-boson wave packets in the unitary gauge and then transform back to obtain the initial conditions in the temporal gauge. The gauge field for a configuration of two well-separated wave packets in the unitary gauge can be written as

$$W^{c,\mu}=W_L^{c,\mu}+W_R^{c,\mu}, \tag{11}$$

with c being the isospin index and μ the Lorentz index. $W_L^{c,\mu}$ is a left-moving wave packet, initially centered at z_L; $W_R^{c,\mu}$ is a right-moving wave packet, initially centered at z_R. In our simulation, z_L and z_R are chosen in such a way that the two wave packets are positioned symmetrically about the center of the lattice. Specifically, we take transversely polarized wave packets

$$W_L^{c,\mu}=(0,0,1,0)n_L^c\psi(z-z_L,-t), \tag{12}$$

$$W_R^{c,\mu}=(0,0,1,0)n_R^c\psi(z-z_R,+t), \tag{13}$$

with n_L^c and n_R^c being the polarization vectors in isospin space. We choose $n_R^c=(0,0,1)$ fixed and leave n_L^c free to be varied. The above choice satisfies the relation $\partial_\mu W^\mu=0$.

Because we have chosen transversely polarized wave packets,[2] they already satisfy the temporal gauge condition $W_0=0$. If we had chosen, instead, longitudinally polarized wave packets (as in Ref. [1]), we would have needed to apply a gauge transformation $U(\mathbf{x},t)$ which transforms W_μ to A_μ,

$$A_\mu=UW_\mu U^{-1}-(1/ig)(\partial_\mu U)U^{-1}, \tag{14}$$

such that $A_0=0$, i.e.,

$$\partial_0 U=igUW_0. \tag{15}$$

In our case, obviously, $U=1$.

To construct the wave packets, we need to specify the functional form of $\psi(\mathbf{x},t)$. A right-moving wave packet centered at $z=0$ at time $t=0$ with mean wave number $\bar{k}$, width Δk, and mean frequency $\bar{\omega}=\sqrt{k^2+M_W^2}$ is described by

$$\psi(z,t)=\frac{\sqrt{\hbar}}{\sqrt{4\pi\sqrt{\pi}\Omega\Delta k\sigma}}\int_{-\infty}^{\infty}dk_z e^{-(k_z-\bar{k})^2/2(\Delta k)^2}\times[e^{i(\omega(k_z)t-k_z z)}+\text{c.c.}], \tag{16}$$

with $\omega(k_z)=\sqrt{k_z^2+M_W^2}$ and

$$\Omega=\bar{\omega}\left\{1+\frac{1}{4}\left[1-\left(\frac{\bar{k}}{\bar{\omega}}\right)^2\right]\left(\frac{\Delta k}{\bar{\omega}}\right)^2+O\left[\left(\frac{\Delta k}{\bar{\omega}}\right)^4\right]\right\}, \tag{17}$$

where the amplitude of the wave packet is fixed by requiring energy equal to $\hbar\bar{\omega}$ (''one particle'') per cross sectional area σ. In the following, we will set $\hbar=1$.

Performing the k_z integral at $t=0$ gives

$$\psi|_{t=0}=\sqrt{\frac{2\Delta k}{\sqrt{\pi}\Omega\sigma}}e^{-(\Delta kz)^2/2}\cos(\bar{k}z). \tag{18}$$

Since the differential equations are of second order in time, one also needs to specify $\dot{\psi}\equiv\partial\psi/\partial t$ at $t=0$, which is found to be

$$\dot{\psi}|_{t=0}=\frac{i}{\sqrt{4\pi\sqrt{\pi}\Omega\Delta k\sigma}}\int_{-\infty}^{\infty}dk_z\omega(k_z)e^{-(k_z-\bar{k})^2/2(\Delta k)^2}[e^{i[\omega(k_z)t-k_z z]}-\text{c.c.}]_{t=0}$$
$$=\sqrt{\frac{2\bar{\omega}\Delta k}{\sqrt{\pi}\sigma(\Omega/\bar{\omega})}}e^{-(\Delta kz)^2/2}\left\{\sin(\bar{k}z)+\frac{\bar{k}}{\omega}\frac{\Delta k}{\omega}\Delta kz\cos(\bar{k}z)+\frac{1}{2}\left[1-\left(\frac{\bar{k}}{\omega}\right)^2\right]\left(\frac{\Delta k}{\omega}\right)^2[1-(\Delta kz)^2]\sin(\bar{k}z)+O\left[\left(\frac{\Delta k}{\omega}\right)^3\right]\right\}. \tag{19}$$

Furthermore, the initial condition for the Higgs field is chosen as the vacuum solution

$$\phi^0=v,\quad \phi^a=0,\quad \dot{\phi}^0=\dot{\phi}^a=0\quad \text{at } t=0. \tag{20}$$

To determine the number of independent parameters, we make use of the scaling transformation (4) for $\psi|_{t=0}$. In terms of the primed quantities, Eq. (18) reads

$$\psi'|_{t'=0}=(1/v)\psi|_{t=0}=(1/\pi^{1/4})\sqrt{\frac{\Delta k/M_W}{(\Omega/M_W)(\sigma M_W^2/g^2)}}e^{-(\Delta k/M_W)^2z'^2/4}\cos[(\bar{k}/M_W)z'/\sqrt{2}], \tag{21}$$

[2]Note that under realistic conditions, the luminosity for transversely polarized gauge bosons in proton-proton system is typically two orders of magnitude higher than for longitudinally polarized ones and increases with energy [17].

where

$$\frac{\Omega}{M_W}=\sqrt{1+(\bar{k}/M_W)^2}\left[1+\frac{1}{4}\frac{(\Delta k/M_W)^2}{[1+(\bar{k}/M_W)^2]^2}+O((\Delta k/\bar{k})^4)\right]. \tag{22}$$

The above initial condition contains three dimensionless parameters: $\bar{k}/M_W$, $\Delta k/M_W$, and $\sigma M_W^2/g^2$. There appears one more parameter in the initial condition, i.e., the relative rotation in isospin space between the two wave packets, which we denote by θ_C.

Combining equations of motion and initial condition, our ansatz has five independent parameters: M_H/M_W, $\bar{k}/M_W$, $\Delta k/M_W$, $\sigma M_W^2/g^2$, and θ_C. The parameter $\bar{k}/M_W$, which sets the energy of collisions in units of the W-boson mass, is referred to as the energy parameter. $\Delta k/M_W$, whose inverse specifies the width of each wave packet in position space, can be called the width parameter. The amplitude of each wave packet depends on $\bar{k}/M_W$ as well as $\Delta k/M_W$, but more crucially, on $\sigma M_W^2/g^2$. In our simulation, we always require $\bar{k}\gg\Delta k$ so that the wave packets are well-defined objects. Furthermore, we choose $\bar{k}\gg M_W$ to model high energy scattering.

In our numerical calculations, the SU(2) coupling constant g was fixed to be 0.65. However, because of the scaling properties of the equations of motion and the initial conditions, the results of our calculation do not depend on the particular choice of g and v. This can be verified by the fact that the amplitude of the wave packets only depends on the ratio of σ and g^2. Also, since the dynamics does not depend on a particular choice of σ or g as long as the ratio σ/g^2 is fixed (assuming that M_W and other parameters remain fixed), we can predict, from the result for one coupling g at a certain value of σ, the result for another coupling g' at a different $\sigma'=(g'/g)^2\sigma$. Hence, a change of the value for the gauge coupling g simply corresponds to a rescaling of the parameter σ controlling the amplitude of initial wave packets.

III. NUMERICAL RESULTS

A. Dependence on the mass ratio M_H/M_W

As established in the previous work [4], the behavior of the wave packet collisions is governed by the nonlinearity because of the self-interaction of the gauge field. For two wave packets of parallel isospin polarizations in the pure Yang-Mills theory, where the nonlinear self-coupling in the gauge field is absent, we found no indication of any interaction [4]. This provided a check on our numerical procedure and showed that the artificial interactions introduced by the formulation in terms of compact lattice gauge fields did not affect the results.

Here, for the Yang-Mills-Higgs system, the situation is more involved. Besides the nonlinearities because of the gauge field self-interaction, there exist other nonlinearities induced by the gauge-Higgs coupling and by the Higgs self-interaction. However, in the case where most energy remains contained in the gauge field and the Higgs field is only slightly excited, one can expect that the gauge field self-interaction will be the major contributor to the nonlinearities observed in the system. Note that the amplitudes of the gauge and Higgs fields shown in the figures below are in the temporal gauge. This means that the longitudinal part of the gauge field is not fully represented in the figures.

The top rows of Figs. 1 and 2 show a few ''snapshots'' of the space-time development of the colliding W-boson wave packets with $M_H=M_W=0.126$, $\sigma=0.336$, $\bar{k}=\pi/5$, and $\Delta k=\pi/100$ for parallel (Fig. 1) and orthogonal (Fig. 2) isospin polarizations, respectively. The figures show the absolute magnitude of the scaled gauge field amplitude, $|\mathbf{A}'|=|\mathbf{A}|/v$. For parallel isospin orientations, the result of the ''collision'' is a slight distortion of the initial wave packets showing no sign of significant inelasticity. In contrast, the top row of Fig. 2 illustrates that the collision of two wave packets with orthogonal relative polarizations in isospin space is strongly inelastic.

The difference between the two figures is even more clearly illustrated by looking at the evolution of the absolute value of the Fourier transform of the gauge-invariant energy density (scaled by v^2)

$$\tilde{\mathscr{E}}(\mathbf{k},t)=\frac{\mathscr{E}(\mathbf{k},t)}{v^2}=\frac{1}{4v^2}\left|\int d^3x\ e^{i\mathbf{k}\cdot\mathbf{x}}\mathrm{Tr}[\mathbf{E}^2(\mathbf{x},t)+\mathbf{B}^2(\mathbf{x},t)]\right|, \tag{23}$$

where $\mathbf{E}$ is the gauge electric field and $\mathbf{B}$ the gauge magnetic field. It is seen that the spectrum for the parallel isospins (median row in Fig. 1) does not change its shape dramatically, while for the case of orthogonal isospins (median row in Fig. 2), the spectrum spreads out widely. The spike at $k=0$ in these spectra corresponds to the total energy contained in the transverse gauge field. From its slight decrease in Fig. 2, we see that the energy transferred to the Higgs and the longitudinal gauge fields during the collision is small ($\approx 10\%$). This reflects the fact that the nonlinearity due to the gauge field self-coupling dominates. Furthermore, the bottom rows of Figs. 1 and 2 illustrate the time evolution of the Higgs field excitations[3] around its condensate value v (which is scaled to unity) accompanying the collision process shown in the top rows of Figs. 1 and 2. Here, we have plotted the square $|\Phi'|^2=|\Phi|^2/v^2$ of the Higgs field as a function of space coordinate at three different times. Throughout our simulations, we have kept $k_{\min}\ll\Delta k\ll k\ll k_{\max}$, where $k_{\min}$ and $k_{\max}$ are the minimum and maximum momentum on the lattice, respectively. This ensures that the wave packets are smooth on the lattice. But during collisions, unlike quantum mechanics, classical dynamics does not provide a mechanism for stopping power from flowing to very low frequency modes (close to $k_{\min}$) or to very high frequency modes (close to $k_{\max}$). In our calculations, the power flowing to high frequency modes does not cause a deterioration in the local smoothness of the gauge field at the end of the simulations.

[3]As seen from (9), oscillations of the gauge boson field act as a source for Higgs field excitations. The Eq. (8) for the gauge field does not possess a source term.

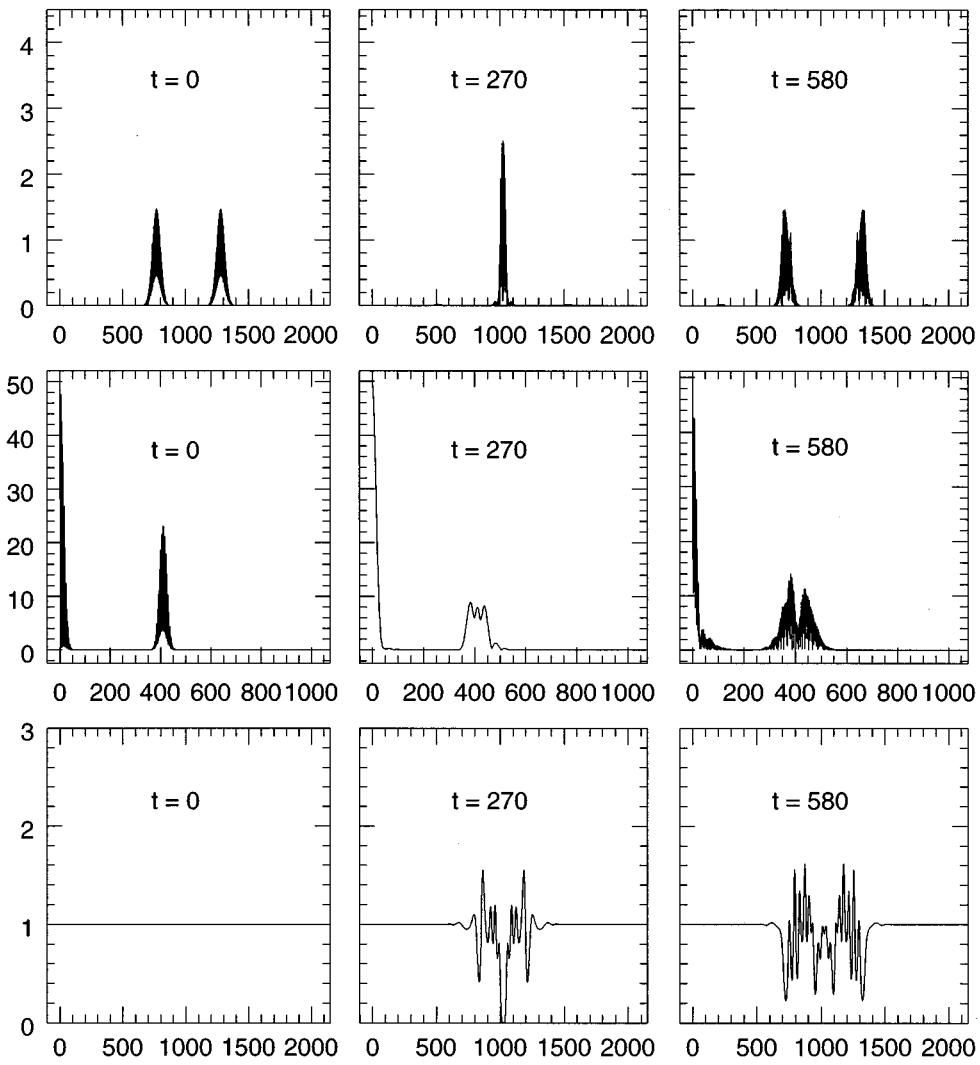

FIG. 1. Collision of two W-wave packets with parallel isospin polarizations. We choose $M_H=M_W=0.126$, $\bar{k}=\pi/5$, $\Delta k=\pi/100$, $g=0.65$, and $\sigma=0.336$. This simulation, as well as all others below, was performed on a lattice of length $L=2048$ and lattice spacing $a=1$. The top row shows the space-time evolution of the scaled gauge field amplitude $|\mathbf{A}'|$, the median row exhibits the corresponding Fourier spectra of the gauge field energy density, Eq. (23), and the bottom row shows the space-time evolution of the scaled Higgs field $|\Phi'|^2$. The abscissae of top and bottom rows are labeled in units of the lattice spacing, and the abscissa of the median row is in units of $\pi/1024$.

To display dependence on the mass ratio $r=M_H/M_W$, the top row of Fig. 3 shows the collision of two orthogonally polarized W-wave packets at the final time ($t=580$) for three different values of $r=M_H/M_W$. It is seen that the ''inelasticity'' is more pronounced for small r. On the other hand, the distortions in the wave packets still survive at large r (even at $r=100$, not shown here). This can be understood as follows. Remember that there are three sources of nonlinearity, namely, gauge field self-coupling, gauge-Higgs coupling, and Higgs self-coupling. As the Higgs mass increases, the Higgs modes begin to decouple. As a result, the interaction between gauge and Higgs fields diminishes and hence contributes less to the nonlinear effects. The gauge field self-interaction is not affected by the change in the Higgs mass and acts as the main contributor of nonlinear effects observed during the collision. The median row of Fig. 3 is the analogue of the top row of Fig. 3 in momentum space, as defined in (23). Again, it gives a clearer picture of the inelasticity of the collision process. The bottom row of Fig. 3 demonstrates that the amplitude of the Higgs field excitations becomes smaller as the Higgs boson mass is increased, while their frequency increases with M_H.

It is remarkable that for small Higgs boson mass, as seen for $r=0.1$ in Fig. 3, the Higgs field oscillates not about the vacuum expectation value v but rather about zero. This observed behavior holds even at larger values of r, up to $r\approx 0.5$ (not shown here). This suggests that for not too large r, the collision of gauge field wave packets, accompanied by energy transfer from gauge field to Higgs field, leads to restoration of the broken symmetry. This phenomenon occurs for gauge field configurations with large amplitudes.[4] Indeed, it is easy to see that $\rho=-\sqrt{2}v$ (i.e., $|\Phi|=0$) is an exact

[4]The idea that the restoration of vacuum symmetry is possible in the background of intense gauge fields was first noted in [18]. Also see [19], where the role of external gauge fields in the restoration of broken symmetries was considered.

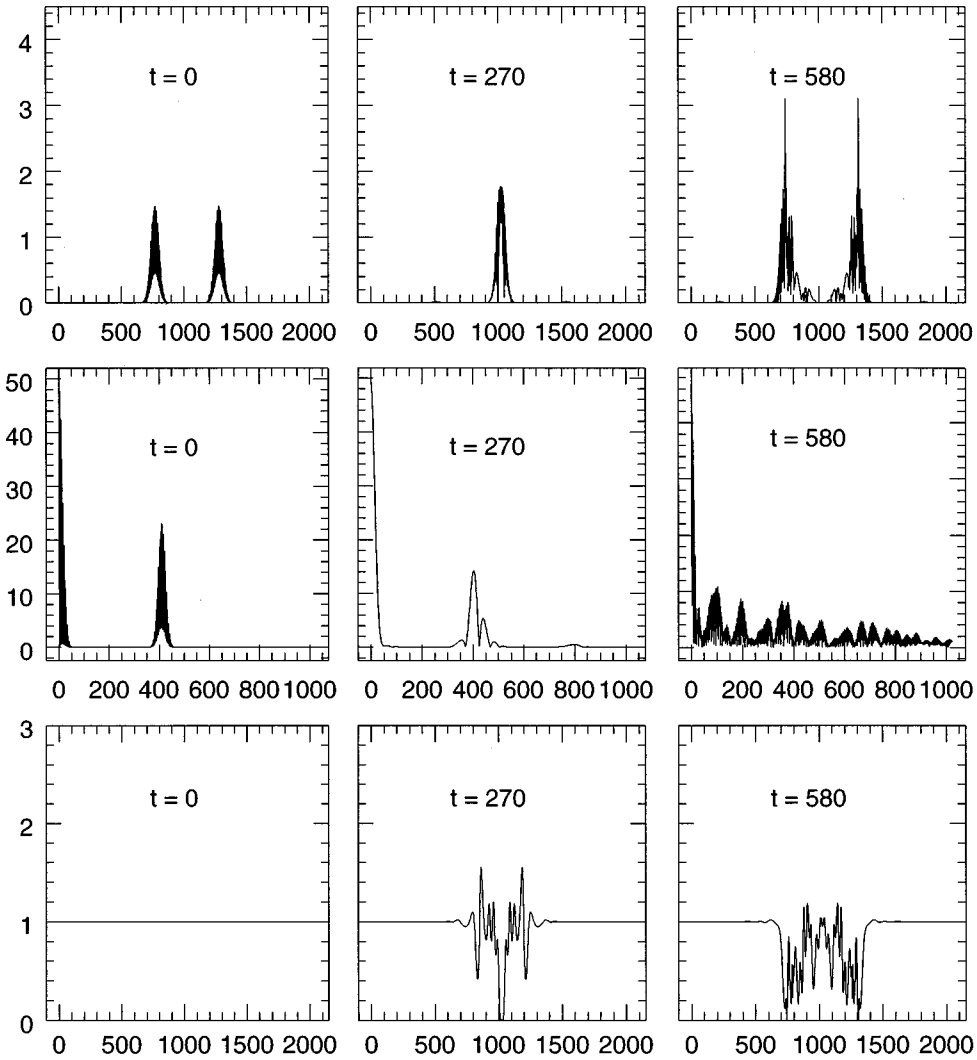

FIG. 2. Same as Fig. 1, but for orthogonal isospin polarizations.

solution to Eq. (9). Inserting $\rho=-\sqrt{2}v$ into Eq. (8) leads to the pure Yang-Mills equation for massless W bosons. In terms of excitations around this state, $\chi=\rho+\sqrt{2}v$, we rewrite Eqs. (8) and (9) as

$$[D_\mu,F^{\mu\nu}]+\tfrac{1}{4}g^2\chi^2W^\nu=0, \tag{24}$$

$$\left[\partial_\mu\partial^\mu-\frac{1}{2}M_H^2\left(1+\frac{g^2W^2}{8\lambda v^2}\right)\right]\chi+\lambda\chi^3=0, \tag{25}$$

where $W^2=-(W_i^a)^2<0$ for transverse polarized wave packets (the sum over spatial index i and isospin index a is assumed here and below). After dropping a constant term λv^4, the corresponding effective potential describing the excitations χ has the form

$$V(\chi,W_\mu)=-\lambda v^2(1-\eta)\chi^2+\frac{\lambda}{4}\chi^4, \tag{26}$$

where we denote

$$\eta\equiv\frac{g^2(W_i^a)^2}{8\lambda v^2}=\frac{1}{r^2}\left(\frac{W_i^a}{v}\right)^2. \tag{27}$$

In the following, we use η as a parameter in which the true intensity $(W_i^a)^2$ of the high frequency gauge field pulses is replaced by its space-time average $\langle W^2\rangle$. Depending on whether $\eta<1$ or $\eta>1$, the potential (26) has two different *stable* minima:

$$\text{for } \eta<1,\quad \chi_{\min}=\pm\sqrt{2}v(1-\eta)^{1/2},\ \text{i.e.,}\ |\Phi|=v(1-\eta)^{1/2}, \tag{28}$$

$$\text{for } \eta\geqslant 1,\quad \chi_{\min}=0,\quad \text{i.e.,}\ |\Phi|=0. \tag{29}$$

Stable excitations about these ''vacua'' have the squared masses

$$\tilde{M}_W^2=M_W^2(1-\eta)\,\theta(1-\eta), \tag{30}$$

$$\tilde{M}_H^2=\frac{M_H^2}{2}|1-\eta|[1+\theta(1-\eta)]. \tag{31}$$

Thus, for $\eta>1$, the broken symmetry is restored and oscillations of the scalar field occur about the symmetrical state $|\Phi|=0$, not about $|\Phi|=v$. The effective mass of the gauge bosons in the region where the symmetry is restored van-

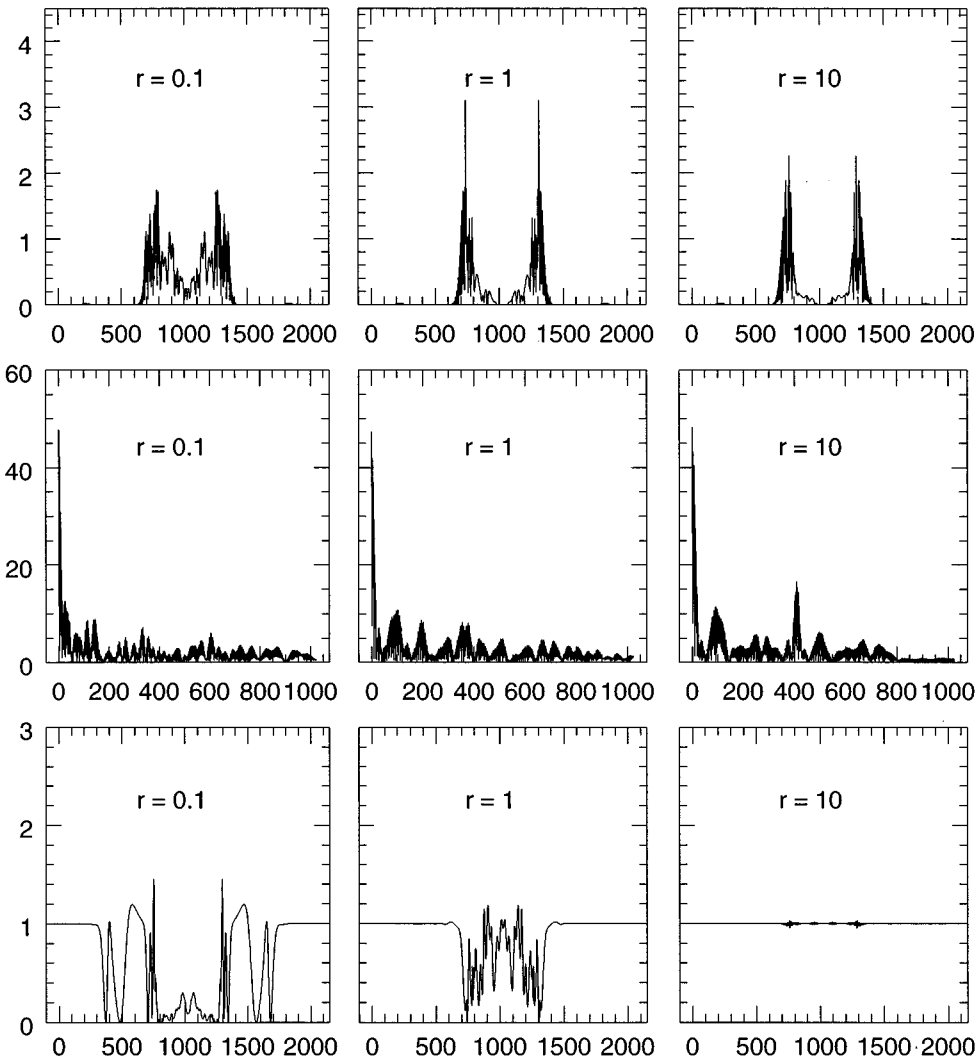

FIG. 3. Mass ratio $r=M_H/M_W$ dependence of the collisions shown for three different values of r at the end of our calculation ($t=580$). Here, we have used orthogonally polarized W-wave packets. Except the mass of the Higgs boson, all the other parameters are fixed to be the same as in Fig. 1.

ishes. For $\eta<1$, the ratio between the effective masses $\tilde{M}_H$ and $\tilde{M}_W$ has no dependence on η and remains $r=M_H/M_W$. Relations (30) and (31) are characteristics of a second order phase transition. The expression (27) for η shows that in the regime of large $(W_i^a)^2>v^2$, this phase transition can occur for experimentally favorable mass ratio $r>1$.

Oscillations of the scalar field around the new symmetrical minimum $|\Phi|=0$ are clearly seen for $r=0.1$ where $\eta\approx 126$ (see Fig. 3). These numerical results provide indications for transition from the phase with spontaneously broken SU(2) symmetry and asymmetric vacuum to the phase with restored SU(2) symmetry and symmetric vacuum as a result of the collisions. Since η is the only relevant parameter in question here, this transition can occur either for small λ (light Higgs boson) or for large λ (heavy Higgs boson) if amplitude of the gauge field is large enough. In Fig. 3, it is also interesting to notice that the spatial region showing symmetry restoration seems to be wider than the region where the colliding wave packets stay visibly large.

It is clear that the phenomenon discussed above does not depend on the one-dimensionality of space in our calculations. However, it is to be expected that the symmetry restoration would not persist as long in three dimensions as the wave packets disperse more rapidly after the collision, causing the squared amplitude $\langle W^2\rangle$ to decay more rapidly.

B. Yang-Mills and BPS limit

In the light of the previous work [4], it is instructive to study the limiting case of the present system as $M_H, M_W\to 0$ while fixing $r=M_H/M_W$ (which is chosen to be one here). Of course, this corresponds to the limit $v\to 0$, where one expects that the gauge field in the Yang-Mills-Higgs system behaves most closely to that in a pure Yang-Mills system. In Fig. 4, the top row shows snapshots of the collision of two orthogonally polarized wave packets with $M_H=M_W=0.001$ and the bottom row exhibits the corresponding spectra. Qualitatively, these figures show that the time evolution is very similar to that seen in the pure Yang-Mills system (see Figs. 2 and 4 in [4]).

The second interesting limit is the Bogomol'ni-Prasad-Sommerfield (BPS) limit [20] where $M_H\to 0$ but M_W is fi-

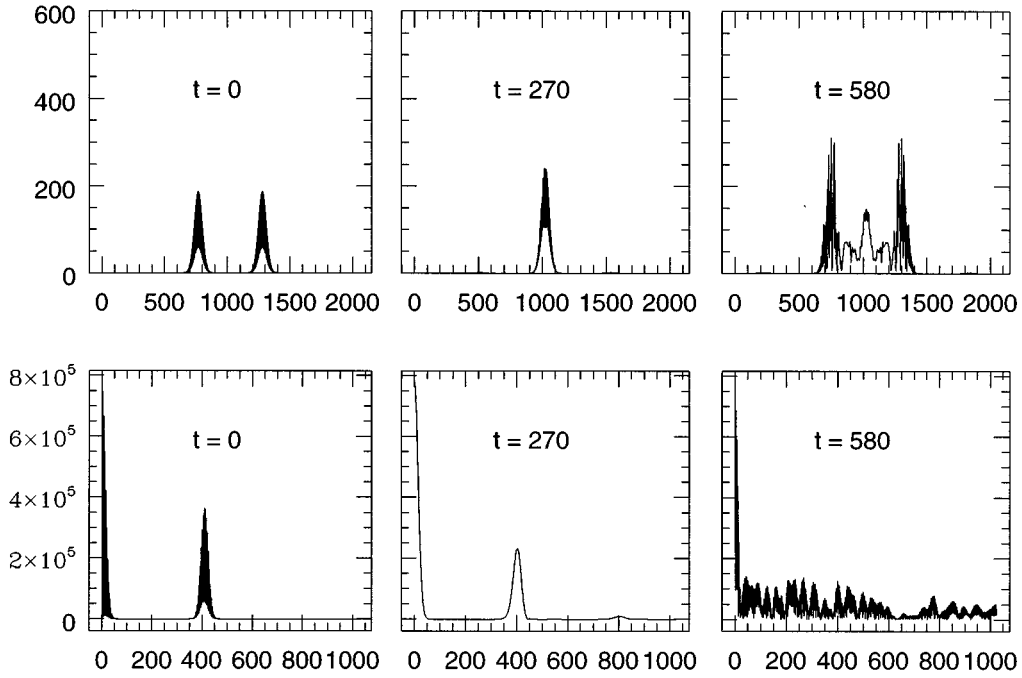

FIG. 4. Collision of two orthogonally polarized wave packets in the Yang-Mills limit. Except for $M_H = M_W = 0.001$, all the other parameters are the same as in Fig. 1. The top row shows the space-time evolution of the scaled gauge field amplitude. The bottom row shows the Fourier spectra of gauge field energy density, as defined in (23).

nite ($\lambda \to 0$, v fixed). Figure 5 shows the snapshots and spectra for this case with $M_W = 0.126$ and $r = 0.01$. Again, we display only the orthogonal case, which reveals complete destruction of the wave packets as in the pure Yang-Mills limit. It is interesting to note that in this limit, the static force between equally charged W bosons vanishes because of the precise cancellation between the photon and (massless) Higgs exchange diagrams, which is a result of the electromagnetic duality [21]. For a pair of oppositely charged W bosons, the contributions from these diagrams add to each other, doubling the attraction.

C. Dependence on the initial amplitude and energy

In our simulation, the most crucial role is played by the initial amplitude of the wave packets. As in the pure Yang-Mills case [4], we find that the amount of ''inelasticity'' observed in the present system is closely linked to the magnitude of the dimensionless amplitude (21). This amplitude depends on several independent parameters: $\sigma M_W^2/g^2$, $\Delta k/M_W$, and $\Omega/M_W \approx \bar{k}/M_W$ (for $\bar{k} \gg M_W$), each of which has a different physical meaning. Noting that the gauge coupling constant is fixed to be $g = 0.65$ throughout our simulation and M_W is a fixed quantity in reality, the best way to study the amplitude dependence is to vary σ without changing anything else. By varying σ, we find that the nonlinear effects increase with amplitude. For a very large σ (very small amplitude), we find no indication of ''inelasticity'' in the colliding wave packets at the end of the simulation.

To search for the energy dependence, we have to study the dependence on $\bar{k}$, which determines the energy of the initial wave packet. In the meantime, we fix σ, M_W, and M_H. M_W and M_H are chosen to be much smaller than $\bar{k}$ to model high energy scattering. Furthermore, as we change $\bar{k}$, Δk is either fixed or changed proportionally to fix the ratio $\Delta k/\bar{k}$. In Fig. 6, we display snapshots of collisions at the final time for different sets of $\bar{k}$ and Δk. Figure 7 shows the corresponding spectra. The orthogonal isospin cases in Figs. 6 and 7 are shown in the left column with their parallel isospin counterparts in the right column.

Clearly, the observed nonlinear effects in the orthogonal cases are qualitatively similar for different $\bar{k}$ or Δk; while in the parallel cases, regardless of Δk, the nonlinear effects disappear as $\bar{k}$ is increased from $\pi/25$ to $\pi/5$.

IV. DISCUSSIONS

A. Amplitude dependence

Our numerical calculations show, for a wide range of parameters, that the wave packet collisions with orthogonal isospin orientation are strongly inelastic if the scaled initial amplitude [see Eq. (21), $\bar{k} \gg M_W$]

$$\left(\frac{2\Delta k}{\sqrt{\pi}\bar{k}\sigma v^2} \right)^{1/2} \tag{32}$$

is of the order of unity. We recall that the expression (21) for the scaled amplitude was determined by the condition that the wave packet contains one particle per transverse area σ.

Although, in the strict sense, our configurations describe wave packets which are infinitely extended in the transverse direction and hence contain infinitely many particles, only a finite transverse area influences the dynamics over a finite period of time. As argued in [4], causality restricts that area to $\sigma(T_s) = \pi T_s^2$ where T_s is the elapsed time after the impact of the two wave packets. The relevant number of particles in the initial state is therefore given by

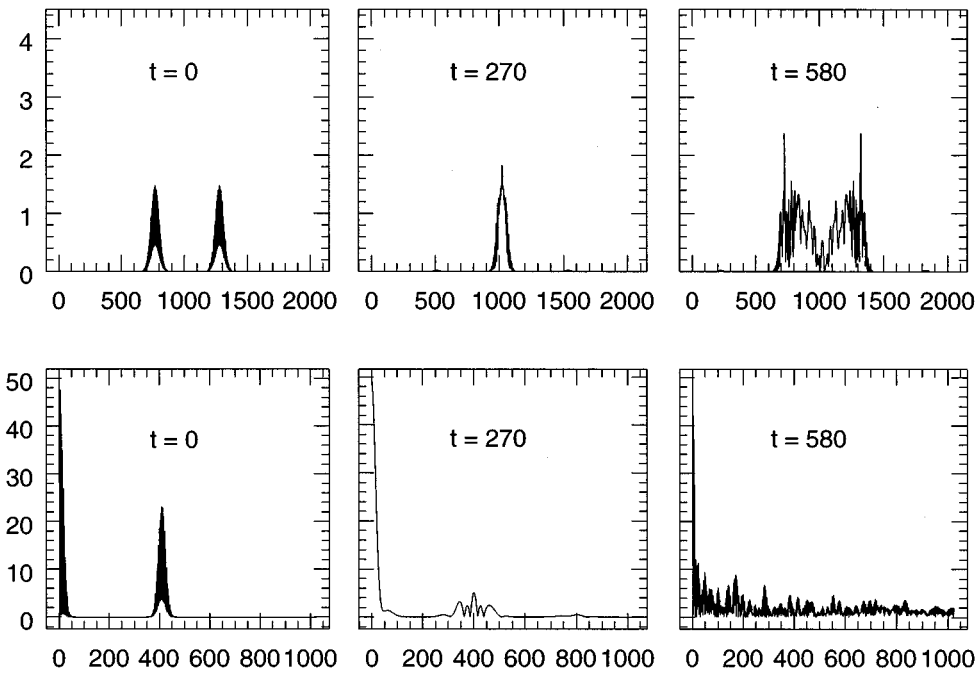

FIG. 5. Collision of two orthogonally polarized wave packets in the BPS limit. Here, we fix $M_W=0.126$ but choose a small mass for the Higgs: $M_H=10^{-2}M_W$. All the other parameters are the same as in Fig. 1. The top row shows the space-time evolution of the scaled gauge field amplitude. The bottom row shows the Fourier spectra of gauge field energy density, as defined in (23).

$$N_i^{\rm eff}=\frac{\sigma(T_s)}{\sigma}=\frac{\pi T_s^2}{\sigma}. \tag{33}$$

What is the lower bound on $N_i^{\rm eff}$ under realistic conditions, for which strongly inelastic events occur? Let us first estimate the constraints on our parameters from a realistic point of view. Clearly, we must have $k\gg v$. The natural spread of any W-boson wave packet produced in high energy interactions is of order $\Delta k\sim v$ in the comoving reference frame. Therefore, the typical transverse area of the W-boson wave packet is of order $\sigma\approx 1/v^2$. Because of Lorentz contraction, its longitudinal momentum spread will generally be much larger than v, or of order $\Delta k_\parallel\sim\gamma v$, where $\gamma\approx k/M_W$ is the Lorentz factor. As a result, $\Delta k_\parallel/k$ will be approximately independent of the collision energy, with a value not much smaller than one. Assuming, e.g., $\Delta k/k\approx 0.5$ in (32), we obtain an amplitude of order unity implying that a few W bosons per area σ in the initial state could produce strong inelasticity. Of course, the precise lower bound on the particle number will depend on the detailed shape of the wave packets and requires a full three-dimensional analysis. But our estimate shows that strongly inelastic events are not excluded for collisions of wave packets containing few particles. In this respect, the results of our analysis correspond to those of Rebbi and Singleton [10] who found that few-particle initial states may not be excluded for baryon number nonconserving processes resulting in multiparticle final states.

As mentioned above, the finite transverse size of order v^{-1} limits the applicability of our calculation for the real three-dimensional case to times $T_s\leqslant v^{-1}$. Since the inelasticity is clearly revealed for times $T_s\sim 100$ (see, e.g., Fig. 5), our numerical results apply most confidently to very high energy where $k/v\geqslant 10^2$.

B. Energy dependence

We now turn to the question of the energy dependence of the nonlinear effects seen in the wave packet collisions. In the $(1+1)$-dimensional Abelian Higgs model, the nonlinearities were clearly found to decrease with energy [1]. For the non-Abelian Higgs model discussed here, the answer is given in Figs. 6 and 7. The inelasticity seen in the orthogonal isospin cases does not change significantly with energy, while it dies out in the parallel isospin cases as k increases. This shows the fundamental role of the non-Abelian nature of the W-W interaction in the formation of strongly inelastic final states.

From Figs. 6 and 7 one can also see that the inclusion of the Higgs field produces new phenomena which are not seen in the pure Yang-Mills system: For initial configurations with parallel isospin, in which case nonlinear interactions of the gauge bosons are absent, lowering of the parameter k leads to inelastic final states. This is exclusively because of the Higgs field since the collision of wave packets with parallel isospin configurations in the pure Yang-Mills theory always leads to elastic final states independently of k [4]. Of course, this pattern indicates that the influence of the Higgs coupling to the gauge field increases for smaller k. How does one understand this behavior? For this purpose, we recall that all our calculations are in the regime of high energy $(k\gg v, M_W)$. For the highest energy of the collisions $(k=\pi/5)$, where parallel polarized wave packets scatter elastically, one may think that the transversely polarized W-W

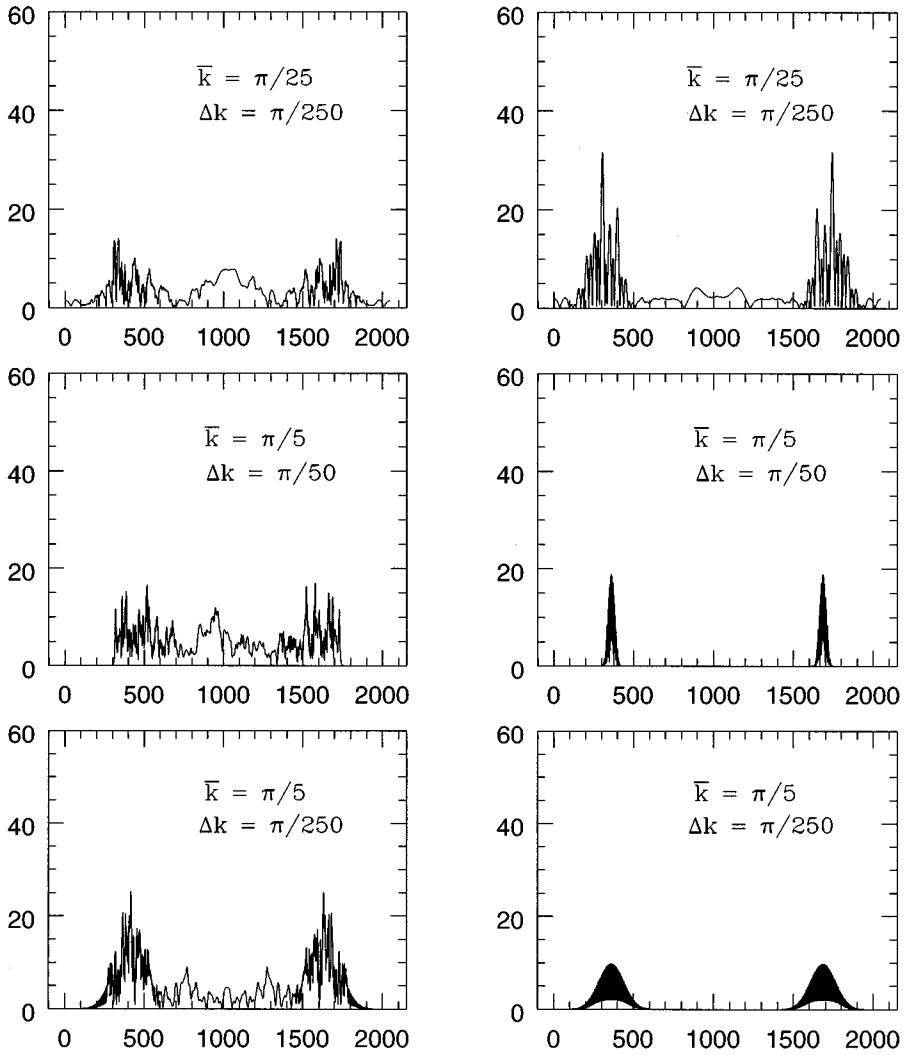

FIG. 6. Final states ($t=1100$) of the scaled gauge field for three different sets of $\bar{k}$ and Δk are shown. Here, $\sigma=0.504$ and $M_H=M_W=0.01$, while all the other parameters are the same as in Fig 1. Left column: orthogonal isospin orientations. Right column: parallel isospin orientations.

scattering (elastic in these collisions) proceeds via exchanges of the gauge and of the Higgs bosons in the tree approximation. The first contribution prevails at high energy, but it does not contribute to the inelastic final states for the parallel isospin orientation. Inelasticity may arise here only from the nonlinear coupling of the gauge and Higgs fields or, in diagrammatic language, because of the Higgs exchange whose contribution increases with the lowering of $\bar{k}$.

V. CONCLUSION

We have numerically studied collisions between classical wave packets of transversely polarized gauge bosons in the spontaneously broken Yang-Mills-Higgs theory. Our main results are the following.

(1) We have found evidence for the creation of final states with dramatically different momentum distributions (strongly ''inelastic'' events) for a wide range of the essential parameters.

(2) These inelastic events persist at the highest investigated energies ($\bar{k}/M_W\sim 10^2$) for collisions with orthogonal isospin polarization, reflecting the essentially non-Abelian character of the interaction. For parallel isospin configurations, in contrast, the inelastic events, which are solely because of the Higgs field, occur only for lower energies.

(3) Under more realistic conditions as discussed in Sec. IV A, the inelastic events are not excluded for initial configurations with few particles.

(4) We have observed, at least for $r\leqslant 0.5$ (with fixed amplitude for the gauge field wave packets), the phenomenon of symmetry restoration as a result of the wave packet collisions. This transition from the asymmetrical state to the symmetrical one is governed by a single parameter η, which depends on both the mass ratio r and the amplitude of the wave packets.

Summarizing, we conclude that the introduction of the Higgs field (in the broken symmetry phase) does not in general spoil the inelasticity of the final state in collisions with

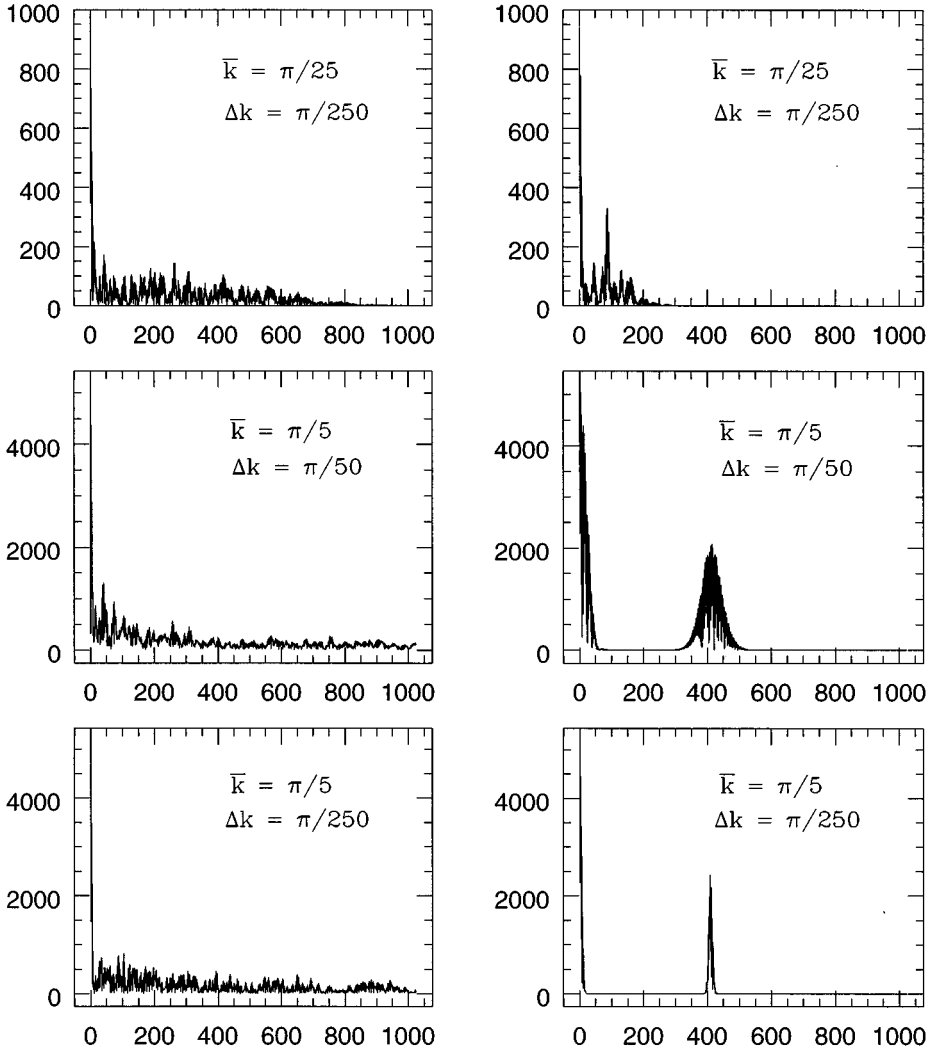

FIG. 7. Energy spectra for the cases shown in Fig. 6.

orthogonal isospin orientation. Our results provide a strong motivation for exploring related phenomena in (3+1) dimensions. This would allow one to study collision between realistically-shaped wave packets and investigate the particle number content of inelastic final states. Last, but not the least, it would be interesting to study the winding number change associated with these collisions.

ACKNOWLEDGMENTS

We thank S. D. H. Hsu and K. Rajagopal for discussions and useful comments. This work was supported in part by Grant Nos. DE-FG05-90ER40592 and DE-FG02-96ER40945 from the U.S. Department of Energy, and by the North Carolina Supercomputing Center.

[1] K. Rajagopal and N. Turok, Nucl. Phys. **B375**, 299 (1992).
[2] H. Goldberg, D. Nash, and M. T. Vaughn, Phys. Rev. D **46**, 2585 (1992).
[3] C. Gong, S. G. Matinyan, B. Müller, and A. Trayanov, Phys. Rev. D **49**, 607 (1994).
[4] C. R. Hu, S. G. Matinyan, B. Müller, A. Trayanov, T. M. Gould, S. D. H. Hsu, and E. R. Poppitz, Phys. Rev. D **52**, 2402 (1995).
[5] A. Ringwald, Nucl. Phys. **B330**, 1 (1990); O. Espinosa, *ibid*. **B343**, 310 (1990).
[6] G. 't Hooft, Phys. Rev. D **14**, 3432 (1976).
[7] M. Voloshin, in *Proceedings of the 27th International Conference on High Energy Physics*, Glasgow, Scotland, 1994, edited by P. J. Bussey and I. G. Knowles (IOP, London, 1995).
[8] V. Rubakov, D. Son, and P. Tinyakov, Phys. Lett. B **287**, 342 (1992).
[9] T. M. Gould, S. D. H. Hsu, and E. R. Poppitz, Nucl. Phys. **B437**, 83 (1995).
[10] C. Rebbi and R. Singleton, in *1994 Summer School in High Energy Physics and Cosmology*, Proceedings, Trieste, Italy, 1994 (World Scientific, Singapore, 1995).
[11] S. G. Matinyan, G. K. Savvidy, and N. G. Ter-Arutyunyan-

Savvidy, Sov. Phys. JETP **53**, 421 (1981); S. G. Matinyan, Sov. J. Part. Nucl. **16**, 226 (1985).
[12] B. Müller and A. Trayanov, Phys. Rev. Lett. **68**, 3387 (1992).
[13] S. G. Matinyan, G. K. Savvidy, and N. G. Ter-Arutyunyan-Savvidy, JETP Lett. **34**, 590 (1981).
[14] J. Ambjørn, T. Aksgaard, H. Porter, and M. E. Shaposhnikov, Nucl. Phys. **B353**, 346 (1991).
[15] J. Kogut and L. Susskind, Phys. Rev. D **11**, 395 (1975); S. A. Chin, O. S. Van Roosmalen, E. A. Umland, and S. E. Koonin, Phys. Rev. D **31**, 3201 (1985).
[16] C. Gong, Ph.D. thesis, Duke University, 1994.
[17] S. Dawson, Nucl. Phys. **B249**, 42 (1985).
[18] D. A. Kirzhnits and A. D. Linde, Phys. Lett. **B42**, 471 (1972).
[19] I. V. Krive, V. M. Pyzh, and E. M. Chudnovskii, Sov. J. Nucl. Phys. **23**, 358 (1976).
[20] M. K. Prasad and C. M. Sommerfield, Phys. Rev. Lett. **35**, 760 (1975); E. B. Bogomol'ni, Sov. J. Nucl. Phys. **24**, 449 (1976).
[21] C. Montonen and D. Olive, Phys. Lett. B **72**, 117 (1977).